1572 © 1992 *The Chemical Society of Japan* *Bull. Chem. Soc. Jpn.*, *65*, *1572—1580 (1992)* [Vol. 65, No. 6

Preparation and Characterization of $[Co(tp)_2(Me_n\text{-}en)]^+$ (tp=Tropolonate Ion; Me_n-en (n=1—4)=N-Methyl Substituted Ethylenediamine), Inversion and Deuteration at Chiral Nitrogen Centers of $[Co(tp)_2(Me\text{-}en\ or\ Me_3\text{-}en)]^+$, and Crystal Structures of $[Co(tp)_2(N,N\text{-}Me_2\text{-}en)]ClO_4$ and $\Lambda(R)\Delta(S)$-$[Co(tp)_2(Me\text{-}en)]ClO_4$

Masaaki Kojima,* Guilin Ma,†,††† Toshiro Miyamoto,††
Shigeru Ohba,†† and Junnosuke Fujita†
Department of Chemistry, Faculty of Science, Okayama University, Tsushima, Okayama 700
†Department of Chemistry, Faculty of Science, Nagoya University, Chikusa-ku, Nagoya 464-01
††Department of Chemistry, Faculty of Science and Technology, Keio University,
3-14-1, Hiyoshi, Kohoku-ku, Yokohama 223

(Received November 18, 1991)

A series of complexes of the type $[Co(tp)_2(R^1R^2NCH_2CH_2NR^3R^4)]^+$ (tp=tropolonate ion; R^1—R^4=H or CH_3) were prepared and characterized by physicochemical methods. The rates of OH^--catalyzed deuteration (H→D, k_D) and inversion (epimerization, k_{ep}) at the chiral amine nitrogen centers of $[Co(tp)_2(Me\text{-}en\ or\ Me_3\text{-}en)]^+$ (Me-en=N-methylethylenediamine, Me_3-en=N,N,N'-trimethylethylenediamine) in aqueous solutions were measured at 34.0 °C. The k_D and k_{ep} values are, respectively, ca. 10 and ca. 10^3 times as large as those of $[Co(acac)_2(Me\text{-}en\ or\ Me_3\text{-}en)]^+$ (acac=2,4-pentanedionate ion). The reduction (Co^{3+}/Co^{2+}) half-wave potential increases from −0.31 (vs. SCE) for $[Co(tp)_2(en)]^+$ (en=ethylenediamine) to −0.09 V for $[Co(tp)_2(Me_4\text{-}en)]^+$ (Me_4-en=N,N,N',N'-tetramethylethylenediamine) in spite of the expected electron-donating effect of the methyl groups, and the results were ascribed to the steric effect of $-N(CH_3)_2$. This interpretation was supported by the X-ray analysis of $[Co(tp)_2(N,N\text{-}Me_2\text{-}en)]ClO_4$ (N,N-Me_2-en=N,N-dimethylethylenediamine) in which the Co–N(tertiary amine) bond length (2.022(4) Å) is longer than the Co–N(primary amine) one (1.930(3) Å). The crystal data and R value are: Monoclinic, $C2/c$, a=16.558(3), b=13.541(2), c=19.125(3) Å, β=102.62(1)°, V=4184(1) Å^3, Z=8, R=0.044 for 2009 observed unique reflections. The crystal structure of $\Lambda(R)\Delta(S)$-$[Co(tp)_2(Me\text{-}en)]ClO_4$ was also determined. The crystal data and R value are: Monoclinic, $P2_1/a$, a=11.608(5), b=22.754(9), c=7.936(6) Å, β=106.02(7)°, V=2015(2) Å^3, Z=4, R=0.084 for 1057 reflections.

It is known that the rates of OH^--catalyzed deuteration (k_D) at the coordinated amine nitrogen centers increase with an increasing positive charge on the complex.[1] In a previous paper,[2] however, we reported that the rates of deuteration and inversion (epimerization, k_{ep}) at the chiral nitrogen centers of $[Co(acac)_2(Me\text{-}en\ or\ Me_3\text{-}en)]^+$ are unusually slow, the k_D and k_{ep} values being ca. 10^2 and ca. 10^4 times, respectively, as small as those of $[Co(ox)_2(Me\text{-}en\ or\ Me_3\text{-}en)]^-$ (ox=oxalate ion). The rates of similar reactions of the sarcosinate ion in $[Co(sar)(Hbg)_2]^{2+}$ (sar=$CH_3NHCH_2COO^-$; Hbg=biguanide=$NH_2C(=NH)NHC(=NH)NH_2$)[3] are also ca. 10^3—10^4 times as small as those of $[Co(sar)(NH_3)_4]^{2+}$.[4] These results suggest that the rates are largely affected by the nature of coexisting ligands. The small rates of the acac and Hbg complexes may be related to delocalized π-electrons in the chelate rings. Thus it is interesting to compare the rates of $[Co(tp)_2(Me\text{-}en\ or\ Me_3\text{-}en)]^+$ with those of $[Co(acac)_2(Me\text{-}en\ or\ Me_3\text{-}en)]^+$; both complexes belong to the CoN_2O_4-type with the same overall charge.

In this paper, we report the rates of epimerization and deuteration at the chiral nitrogen centers of $[Co(tp)_2(Me\text{-}en\ or\ Me_3\text{-}en)]^+$ and the results are compared with one another and with those of the acac and ox complexes. The paper also describes electrochemistry of the tp complexes and the crystal structures of $[Co(tp)_2(N,N\text{-}Me_2\text{-}en)]ClO_4$ and $\Lambda(R)\Delta(S)$-$[Co(tp)_2(Me\text{-}en)]ClO_4$.

Experimental

$[Co(tp)_3]$. This complex was prepared by a method similar to that of Eaton et al.[5] To a solution of $CoCl_2\cdot 6H_2O$ (5 g, 21 mmol) in water (5 cm^3) was added 30% H_2O_2 (7.5 cm^3). This solution was added to an ice-cold slurry of $KHCO_3$ (15 g) in water (15 cm^3) with stirring. The resulting green solution of $[Co(CO_3)_3]^{3-}$ [6] was filtered. Tropolone (7.7 g, 63 mmol) was added to the filtrate and the mixture was heated at 40 °C for 30 min to yield a green solid. It was collected by filtration, washed with water, and recrystallized from chloroform by the addition of petroleum ether. Yield: 7.1 g. UV (CH_2Cl_2) 622 nm.

$[Co(tp)_2(en)]ClO_4\cdot H_2O$, $\Lambda(R)\Delta(S)$-$[Co(tp)_2(Me\text{-}en)]ClO_4\cdot 0.5H_2O$, $\Lambda(S)\Delta(R)$-$[Co(tp)_2(Me\text{-}en)]ClO_4\cdot H_2O$, $[Co(tp)_2(N,N'\text{-}Me_2\text{-}en)]ClO_4$, $\Lambda(RR)\Delta(SS)$-$[Co(tp)_2(N,N'\text{-}Me_2\text{-}en)]Cl\cdot 0.5H_2O$ (N,N'-Me_2-en=N,N'-Dimethylethylenediamine, $\Lambda(SR)\Delta(RS)$-$[Co(tp)_2(N,N'\text{-}Me_2\text{-}en)]ClO_4\cdot 0.5H_2O$, $\Lambda(SS)\Delta(RR)$-$[Co(tp)_2(N,N'\text{-}Me_2\text{-}en)]ClO_4\cdot H_2O$, $\Lambda(R)\Delta(S)$- and $\Lambda(S)\Delta(R)$-$[Co(tp)_2(Me_3\text{-}en)]ClO_4$, and $[Co(tp)_2(Me_4\text{-}en)]Cl\cdot NaCl\cdot H_2O$. These complexes were prepared by a similar method, and a representative procedure is given for $[Co(tp)_2(en)]ClO_4\cdot H_2O$. Ethylenediamine (0.36 g, 6 mmol) was added to a suspension of $[Co(tp)_3]$ (1.6 g, 3.84 mmol) in tetrahydrofuran (900 cm^3). The mixture was stirred for 12 h at 45 °C and then filtered. The filtrate was diluted with water (2 dm^3), and applied on a column (ϕ4.5

[†††] Present address: Department of Chemistry, Yangzhou Teacher's College, Yangzhou, Jiangsu Province, People's Republic of China.

cm×25 cm) of SP-Sephadex C-25. By elution with 0.1 M NaCl (1 M=1 mol dm^{-3}), a brown and a red (probably [Co(tp)(en)$_2$]$^{2+}$) band developed in this order. The eluate containing the brown band was collected and evaporated to a small volume. Sodium perchlorate was added to the concentrate to yield greenish brown crystals, which were collected by

Table 1. Analytical Data and Colors of the Complexes

Complex (Formula)	Found (Calcd)			Color
	C/%	H/%	N/%	
[Co(tp)$_2$(en)]ClO$_4$·H$_2$O	40.05	3.94	5.81	Greenish brown
($C_{16}H_{20}N_2CoClO_9$)	(40.14)	(4.21)	(5.85)	
$(+)^{\mathrm{CD}}_{530}$-[Co(tp)$_2$(en)]ClO$_4$·H$_2$O	40.07	3.94	5.83	Greenish brown
($C_{16}H_{20}N_2CoClO_9$)	(40.14)	(4.21)	(5.85)	
$\Lambda(R)\Delta(S)$-[Co(tp)$_2$(Me-en)]ClO$_4$·0.5H$_2$O	42.51	4.21	5.74	Green
($C_{17}H_{21}N_2ClCoO_{8.5}$)	(42.21)	(4.38)	(5.79)	
$\Lambda(S)\Delta(R)$-[Co(tp)$_2$(Me-en)]ClO$_4$·H$_2$O	41.54	4.44	5.69	Green
($C_{17}H_{22}N_2ClCoO_9$)	(41.43)	(4.47)	(5.66)	
[Co(tp)$_2$(*N*,*N*-Me$_2$-en)]ClO$_4$	44.16	4.48	5.66	Green
($C_{18}H_{22}N_2ClCoO_8$)	(44.23)	(4.54)	(5.73)	
$\Lambda(RR)\Delta(SS)$-[Co(tp)$_2$(*N*,*N*′-Me$_2$-en)]Cl·0.5H$_2$O	50.02	5.27	6.56	Green
($C_{18}H_{23}N_2ClCoO_{4.5}$)	(49.84)	(5.34)	(6.46)	
$\Lambda(SR)\Delta(RS)$-[Co(tp)$_2$(*N*,*N*′-Me$_2$-en)]ClO$_4$·0.5H$_2$O	43.40	4.51	5.57	Green
($C_{18}H_{23}N_2ClCoO_{8.5}$)	(43.43)	(4.66)	(5.63)	
$\Lambda(SS)\Delta(RR)$-[Co(tp)$_2$(*N*,*N*′-Me$_2$-en)]ClO$_4$·H$_2$O	42.30	4.37	5.44	Green
($C_{18}H_{24}N_2ClCoO_9$)	(42.66)	(4.77)	(5.53)	
$\Lambda(R)\Delta(S)$-[Co(tp)$_2$(Me$_3$-en)]ClO$_4$	45.37	4.74	5.58	Green
($C_{19}H_{24}N_2ClCoO_8$)	(45.39)	(4.78)	(5.57)	
$\Lambda(S)\Delta(R)$-[Co(tp)$_2$(Me$_3$-en)]ClO$_4$	45.29	4.68	5.70	Green
($C_{19}H_{24}N_2ClCoO_8$)	(45.39)	(4.78)	(5.57)	
[Co(tp)$_2$(Me$_4$-en)]Cl·NaCl·H$_2$O	45.12	5.17	5.27	Green
($C_{20}H_{28}N_2ClCoNaO_5$)	(45.38)	(5.33)	(5.29)	

Table 2. Crystal Data, Experimental Conditions, and Refinement Details

	(1) [Co(tp)$_2$(Me$_2$-en)]ClO$_4$	(2) $\Lambda(R)\Delta(S)$-[Co(tp)$_2$(Me-en)]ClO$_4$
Formula weight	488.6	474.6
Crystal system	Monoclinic	Monoclinic
Space group and *Z*	$C2/c$, 8	$P2_1/a$, 4
a/Å	16.558(3)	11.608(5)
b/Å	13.541(2)	22.754(9)
c/Å	19.125(3)	7.936(6)
β/°	102.62(1)	106.02(7)
V/Å	4184(1)	2015(2)
D_m and D_x/Mg m^{-3}	—, 1.57	1.55, 1.56
μ(Mo $K\alpha$)/mm^{-1}	0.991	1.030
Color and shape of crystals	Black tabular	Black tabular
Size of specimen/mm^3	0.20×0.20×0.55	0.10×0.18×0.50
$2\theta_{\max}$/°	50	40
Range of h, k, and l	$-19\leqq h\leqq 19$ $0\leqq k\leqq 16$ $0\leqq l\leqq 22$	$-11\leqq h\leqq 11$ $-21\leqq k\leqq 21$ $0\leqq l\leqq 7$
Systematic absences	hkl, $h+k$ odd; $h0l$, l odd	$h0l$, h odd $0k0$, k odd
Possible space groups	Cc or $C2/c$	$P2_1/a$
Variation in standard reflections $\sum(\lvert F_o\rvert/\lvert F_o\rvert_{\mathrm{initial}})/n$	0.954—1.005 n=5	0.998—1.004 n=5
Number of reflections measured	4130	4059
Number of reflections observed [$\lvert F_o\rvert>3\sigma(\lvert F_o\rvert)$]	2073	2093
Relative transmission factor, A	0.740—0.865	0.826—0.905
Number of unique reflections(R_{int})	2009(0.014)	1057(0.026)
$R(F)$	0.044	0.084
$(\Delta/\rho)_{\max}$/e Å^{-3}	0.47	0.46
Number of reflections/number of parameters	5.6	4.1

filtration and recrystallized from methanol by the addition of diethyl ether. Yield: 1.6 g.

The isomers of the Me-en, *N*,*N*′-$\mathrm{Me_2}$-en, and $\mathrm{Me_3}$-en complexes were separated by SE-Toyopearl[7] column chromatography at 0 °C (eluent: 0.05 M NaCl). The chlorides of $\Lambda(RR)\Delta(SS)$-$[\mathrm{Co(tp)_2}(N,N'\text{-}\mathrm{Me_2}\text{-en})]^+$ and $[\mathrm{Co(tp)_2(Me_4\text{-}en)}]^+$ were deposited on evaporating the effluents because of their small solubilities. The other complexes were obtained as the perchlorates in the same way as for $[\mathrm{Co(tp)_2(en)}]\mathrm{ClO_4 \cdot H_2O}$.

The analytical data and colors of the complexes are given in Table 1.

Resolution of $[\mathrm{Co(tp)_2(en)}]^+$. $[\mathrm{Co(tp)_2(en)}]\mathrm{ClO_4 \cdot H_2O}$ (0.479 g, 1 mmol) was converted into the chloride with a Dowex 1X8 anion exchanger in the chloride form. To a hot (ca. 70 °C) aqueous solution (20 $\mathrm{cm^3}$) of $[\mathrm{Co(tp)_2(en)}]\mathrm{Cl}$ was added a hot (ca. 70 °C) solution containing sodium di-*O*-benzoyl-*d*-tartrate (0.201 g, 0.5 mmol) and di-*O*-benzoyl-*d*-tartaric acid monohydrate (0.188g, 0.5 mmol) in 60 $\mathrm{cm^3}$ of water. The mixture was allowed to stand for 30 min at room temperature to yield a brown precipitate. It was collected by filtration and recrystallized from methanol by the addition of diethyl ether. Yield: 0.12 g. The diastereomer was recrystallized from $\mathrm{MeOH\text{-}H_2O}$ repeatedly until no change in the $\Delta\varepsilon$ value was observed. $\mathrm{CD(H_2O)}$ +7.61(18700) and −19.1(24800 $\mathrm{cm^{-1}}$).

The pure diastereomer was dissolved in water and applied on a column (ϕ2 cmX5 cm) of SP-Sephadex C-25. The column was washed with water, and the complex was eluted with 0.2 M NaCl. The complex was isolated as the perchlorate and recrystallized in the same way as for the racemate.

Measurements. Absorption and circular dichroism (CD) spectra were recorded on a Hitachi 323 spectrophotometer and a JASCO J-40CS spectropolarimeter, respectively. ^{1}H NMR spectra were measured with a Hitachi R-90H spectrometer. Electrochemical measurements were performed at 24 °C by using a Fuso HECS 321B potential sweep unit. Rotating disk experiments were carried out on a three-electrode system composed of glassy carbon rotating-disk (2000 rev $\mathrm{min^{-1}}$), platinum-wire, and saturated calomel electrodes as the working, auxiliary, and reference electrodes, respectively. KCl was used as the supporting electrolyte at 0.1 M concentration.

Racemization of $[\mathrm{Co(tp)_2(en)}]^+$. Optically active $[\mathrm{Co(tp)_2(en)}]^+$ was racemized in a phthalate buffer (pH 2.8) and in a phosphate buffer (pH 7.2) at 70 °C, and the decrease in CD strength was recorded in the region of 700—440 nm. In each kinetic run, the plot of ln($\Delta\varepsilon_t$ (530 nm)) vs. time gave a straight line for at least three half-lives, where $\Delta\varepsilon_t$ (530 nm) denotes the CD strength at time *t* and at 530 nm. No change in absorption spectrum was observed during the racemization.

Deuteration Studies. The rates of deuteration at the chiral nitrogen centers of $[\mathrm{Co(tp)_2(Me\text{-}en)}]^+$ and $[\mathrm{Co(tp)_2(Me_3\text{-}en)}]^+$ were measured in a phosphate buffer (pD 6.0—6.9) and a phthalate buffer (pD 5.6—6.7), respectively at 34.0 °C. The

Table 3. Fractional Coordinates and Isotropic Thermal Parameters

Atom	x	y	z	B_{eq} or B_{iso}/Å^2	Atom	x	y	z	B_{eq} or B_{iso}/Å^2
(1)					**(2)**				
Co	0.52239(4)	0.24610(6)	0.62194(4)	3.1	Co	0.7889(2)	0.3672(1)	0.0926(3)	5.5
N(1)	0.6022(2)	0.2569(4)	0.7117(2)	3.9	N(1)A	0.756(2)	0.288(1)	0.169(4)	6.8
N(2)	0.6034(2)	0.3262(3)	0.5800(2)	3.7	N(2)A	0.798(3)	0.320(1)	−0.125(4)	8.8
O(1)	0.5680(2)	0.1248(2)	0.6013(2)	3.7	N(1)B	0.762(2)	0.300(1)	0.210(4)	7.1
O(2)	0.4513(2)	0.1668(2)	0.6630(2)	3.4	N(2)B	0.789(2)	0.316(1)	−0.102(4)	6.1
O(3)	0.4423(2)	0.2472(3)	0.5342(2)	3.6	O(1)	0.6264(8)	0.3836(4)	−0.0061(13)	5.1
O(4)	0.4655(2)	0.3566(2)	0.6458(2)	3.5	O(2)	0.8133(9)	0.4367(4)	−0.0172(14)	5.9
C(1)	0.5284(3)	0.0486(4)	0.6199(3)	3.1	O(3)	0.7946(8)	0.4106(4)	0.2969(13)	4.9
C(2)	0.5543(3)	−0.0453(4)	0.6060(3)	4.9	O(4)	0.9528(9)	0.3555(4)	0.1955(14)	6.1
C(3)	0.5261(4)	−0.1366(4)	0.6222(4)	5.6	C(1)	0.709(2)	0.462(1)	−0.097(2)	5.3
C(4)	0.4624(3)	−0.1603(4)	0.6560(3)	4.7	C(2)	0.722(2)	0.518(1)	−0.185(3)	9.2
C(5)	0.4120(3)	−0.0965(4)	0.6812(3)	4.2	C(3)	0.620(2)	0.554(1)	−0.276(2)	7.1
C(6)	0.4099(3)	0.0056(4)	0.6804(3)	3.5	C(4)	0.495(1)	0.543(1)	−0.301(2)	6.3
C(7)	0.4620(3)	0.0727(4)	0.6548(3)	3.0	C(5)	0.445(1)	0.497(1)	−0.259(2)	5.4
C(8)	0.3857(3)	0.3132(4)	0.5342(3)	3.1	C(6)	0.488(1)	0.447(1)	−0.171(2)	5.1
C(9)	0.3206(3)	0.3224(4)	0.4740(3)	4.0	C(7)	0.603(1)	0.433(1)	−0.096(2)	3.9
C(10)	0.2542(3)	0.3863(5)	0.4607(3)	4.8	C(8)	0.902(1)	0.412(1)	0.407(2)	3.4
C(11)	0.2324(3)	0.4596(5)	0.5030(3)	5.2	C(9)	0.921(2)	0.441(1)	0.561(2)	8.0
C(12)	0.2738(3)	0.4886(5)	0.5704(3)	4.7	C(10)	1.019(2)	0.448(1)	0.707(3)	7.8
C(13)	0.3480(3)	0.4515(4)	0.6116(3)	4.3	C(11)	1.137(2)	0.429(1)	0.724(3)	7.2
C(14)	0.3985(3)	0.3760(4)	0.5977(3)	3.3	C(12)	1.171(2)	0.395(1)	0.610(3)	7.2
C(15)	0.6506(3)	0.3491(4)	0.7080(3)	4.6	C(13)	1.111(1)	0.373(1)	0.437(2)	5.9
C(16)	0.6778(3)	0.3405(4)	0.6387(3)	4.8	C(14)	0.989(1)	0.380(1)	0.348(2)	4.8
C(17)	0.5684(3)	0.4233(4)	0.5534(3)	4.6	C(15)A	0.724(3)	0.250(1)	0.037(4)	4.5
C(18)	0.6262(4)	0.2744(5)	0.5192(3)	5.8	C(16)A	0.823(3)	0.261(2)	−0.075(5)	7.6
Cl	0.1815(1)	0.1431(1)	0.7330(1)	5.3	C(17)A	0.689(2)	0.298(1)	0.260(4)	3.2
O(5)	0.1632(4)	0.1670(4)	0.7982(3)	11.4	C(15)B	0.675(3)	0.255(2)	0.092(6)	8.6
O(6)	0.2006(4)	0.2291(4)	0.7005(3)	11.7	C(16)B	0.767(3)	0.252(1)	−0.050(4)	4.9
O(7)	0.2487(4)	0.0832(5)	0.7481(5)	14.5	C(17)B	0.873(2)	0.324(1)	−0.174(4)	3.7
O(8)	0.1140(4)	0.0991(5)	0.6908(4)	13.6	Cl	0.4870(5)	0.2922(2)	−0.4662(8)	9.1
					O(5)	0.585(2)	0.327(1)	−0.426(3)	18.6
					O(6)	0.507(2)	0.240(1)	−0.396(3)	20.7
					O(7)	0.414(2)	0.319(1)	−0.411(5)	26.0
					O(8)	0.460(2)	0.290(1)	−0.648(2)	23.9

Table 4. Bond Lengths (l/Å) and Bond Angles (ϕ/°) of Complex Cation in (**1**)

Co-N(1)	1.930(3)	N(1)-Co-N(2)	85.8(2)
Co-N(2)	2.022(4)	N(1)-Co-O(1)	91.4(1)
Co-O(1)	1.885(3)	N(1)-Co-O(2)	92.4(1)
Co-O(2)	1.887(4)	N(1)-Co-O(3)	175.1(1)
Co-O(3)	1.898(3)	N(1)-Co-O(4)	90.3(1)
Co-O(4)	1.877(3)	N(2)-Co-O(1)	93.1(1)
N(1)-C(15)	1.494(7)	N(2)-Co-O(2)	177.0(2)
N(2)-C(16)	1.487(6)	N(2)-Co-O(3)	92.3(2)
N(2)-C(17)	1.481(7)	N(2)-Co-O(4)	94.6(2)
N(2)-C(18)	1.476(8)	O(1)-Co-O(2)	84.6(1)
O(1)-C(1)	1.313(6)	O(1)-Co-O(3)	93.2(1)
O(2)-C(7)	1.301(6)	O(1)-Co-O(4)	172.2(1)
O(3)-C(8)	1.295(6)	O(2)-Co-O(3)	89.6(1)
O(4)-C(14)	1.304(6)	O(2)-Co-O(4)	87.7(1)
C(1)-C(2)	1.386(8)	O(3)-Co-O(4)	85.3(1)
C(1)-C(7)	1.443(8)	Co-N(1)-C(15)	106.9(3)
C(2)-C(3)	1.380(8)	Co-N(2)-C(16)	106.4(3)
C(3)-C(4)	1.390(10)	Co-N(2)-C(17)	111.6(3)
C(4)-C(5)	1.360(8)	Co-N(2)-C(18)	111.3(3)
C(5)-C(6)	1.383(8)	C(16)-N(2)-C((17)	109.9(4)
C(6)-C(7)	1.412(8)	C(16)-N(2)-C(18)	110.1(4)
C(8)-C(9)	1.400(7)	C(17)-N(2)-C(18)	107.4(4)
C(8)-C(14)	1.460(8)	Co-O(1)-C(1)	112.4(3)
C(9)-C(10)	1.378(8)	Co-O(2)-C(7)	113.2(3)
C(10)-C(11)	1.378(9)	Co-O(3)-C(8)	111.8(3)
C(11)-C(12)	1.378(8)	Co-O(4)-C(14)	112.6(3)
C(12)-C(13)	1.400(7)	O(1)-C(1)-C(2)	118.4(5)
C(13)-C(14)	1.383(8)	O(1)-C(1)-C(7)	115.1(5)
C(15)-C(16)	1.495(9)	C(2)-C(1)-C(7)	126.5(5)
		C(1)-C(2)-C(3)	130.1(5)
		C(2)-C(3)-C(4)	129.8(6)
		C(3)-C(4)-C(5)	127.2(6)
		C(4)-C(5)-C(6)	130.3(5)
		C(5)-C(6)-C(7)	129.1(5)
		O(2)-C(7)-C(1)	114.5(5)
		O(2)-C(7)-C(6)	118.6(5)
		C(1)-C(7)-C(6)	126.9(5)
		O(3)-C(8)-C(9)	119.2(5)
		O(3)-C(8)-C(14)	115.4(4)
		C(9)-C(8)-C(14)	125.3(5)
		C(8)-C(9)-C(10)	130.3(5)
		C(9)-C(10)-C(11)	130.1(5)
		C(10)-C(11)-C(12)	127.9(5)
		C(11)-C(12)-C(13)	128.3(6)
		C(12)-C(13)-C(14)	130.6(5)
		O(4)-C(14)-C(8)	114.6(5)
		O(4)-C(14)-C(13)	118.1(5)
		C(8)-C(14)-C(13)	127.4(5)
		N(1)-C(15)-C(16)	104.2(4)
		N(2)-C(16)-C(15)	108.6(4)

complex perchlorates were converted into the more soluble chlorides with a Dowex 1×8 anion exchanger in the chloride form. The deuteration reactions were followed with the NMR spectrometer for at least two half-lives. The empirical formula, pD = pH meter reading+0.4, was used to calculate $[OD^-]$.[8)]

Epimerization Studies. Kinetic studies of isomerization (epimerization) between the two isomers ($\Lambda(S)\Delta(R)$ and $\Lambda(R)\Delta(S)$) of $[Co(tp)_2(Me\text{-}en)]^+$ and $[Co(tp)_2(Me_3\text{-}en)]^+$ were performed in a borate buffer (pH 8.5—9.3) and a phosphate buffer (pH 7.3—8.1), respectively, by the high-performance liquid chromatographic method.[9)] The chromatography was carried out with a YMC ODS column (ϕ0.46 cm×25 cm) and 5×10^{-3} M sodium heptanesulfonate in acetonitrile-water (34 : 66 v/v) as the eluent on a JASCO TRI ROTAR V system at a flow rate of 1.0 $cm^3\,min^{-1}$. The complexes were detected with a JASCO UVIDEC-100 IV spectrophotometric detector at 260 nm. Analysis of chromatograms changed with reaction time gives the pseudo first-order rate constant, $k_{cp(obsd)}$. The runs starting from either of the isomers give the same result within the experimental error. From these observations, the reaction can be expressed as

$$\Lambda(S)\Delta(R)\text{ isomer}\underset{k_{-1}}{\overset{k_1}{\rightleftarrows}}\Lambda(R)\Delta(S)\text{ isomer.}$$

The forward and reverse second-order rate constants, k_1 and k_{-1} were obtained from k_{cp} ($k_{cp}=k_1+k_{-1}$) and the equilibrium constant ($k_{eq}=k_1/k_{-1}$).

Crystal-Structure Determination. Crystals of $[Co(tp)_2(N,N\text{-}Me_2\text{-}en)]ClO_4$ (**1**) were obtained by recrystallization from methanol and diethyl ether, and those of $\Lambda(R)\Delta(S)$-$[Co(tp)_2(Me\text{-}en)]ClO_4$ (**2**) were grown from an aqueous $HClO_4$ solution to avoid epimerization. The crystal data, experimental conditions and refinement information are listed in Table 2. The intensities were measured using graphite monochromatized Mo $K\alpha$ radiation (λ=0.71073 Å) on an automated Rigaku four-circle diffractometer AFC-5. The ω scan technique was employed at a scan rate of 6° min^{-1}. The lattice constants were determined from 24 2θ values ($20<2\theta<24°$). Absorption corrections were made by the Gaussian numerical-integration method.[10)] The positions of the heavy atoms were determined by direct methods,[11)] and the other non-hydrogen atoms were located by Fourier syntheses and were refined anisotropically. The H atoms of $[Co(tp)_2(N,N\text{-}Me_2\text{-}en)]ClO_4$ (**1**) were located by the difference syntheses or calculated theoretically and refined with isotropic thermal parameters. There exists orientational disorder of the complex cation in (**2**). The carbon and nitrogen atoms in the Me-en ligand were split into two positions with 50% probability each. These atoms were refined isotropically and the hydrogen atoms were not introduced in the refinement. The function, $\Sigma w||F_o|-|F_c||^2$, was minimized with $w^{-1}=\sigma^2(|F_o|)+(0.015|F_o|)^2$ by the block-diagonal least-squares method. Complex neutral-atom scattering factors were used.[12)] The calculations were carried out on a FACOM M780/10 computer at Keio University using the computation program system UNICS-III.[13)] The final atomic parameters are listed in Table 3, and the bond lengths and bond angles within the complex cation of (**1**) in Table 4.[14)]

Results and Discussion

Preparation and Characterization of the Complexes. The $[Co(tp)_2(diamine)]^+$ complexes were prepared by reaction of $[Co(tp)_3]$ with the diamine ligands in tetrahydrofuran.

The $[Co(tp)_2(en)]^+$, $[Co(tp)_2(N,N\text{-}Me_2\text{-}en)]^+$, and $[Co(tp)_2(Me_4\text{-}en)]^+$ complexes exist in a pair of enantiomers (Λ and Δ), while two ($\Lambda(R)\Delta(S)$ and $\Lambda(S)\Delta(R)$), three, ($\Lambda(RR)\Delta(SS)$, $\Lambda(SR)\Delta(RS)$, and $\Lambda(SS)\Delta(RR)$), and two ($\Lambda(R)\Delta(S)$ and $\Lambda(S)\Delta(R)$) racemic pairs of diastereomers are possible for $[Co(tp)_2(Me\text{-}en)]^+$, $[Co(tp)_2(N,N'\text{-}Me_2\text{-}en)]^+$, and $[Co(tp)_2(Me_3\text{-}en)]^+$, respectively, because of occurrence of chiral nitrogen atoms (R and S) (Fig. 1). All these diastereomers were separated by

SE-Toyopearl column chromatography at 0 °C. The structures of the complexes were assigned on the basis of the chemical shift of the *N*-methyl group in the ^{1}H NMR spectra taking a shielding effect by the tp chelate ring into consideration; an isomer which shows a doublet due to the *N*-methyl protons at a higher magnetic field is assigned to the $\Lambda(S)\Delta(R)$ isomer (Fig. 1 and Table 5).

Table 5 shows the distributions of the isomers at equilibrium (34 °C) and the absorption spectral data for the complexes. The isomers in which the *N*-methyl group is situated over the tp chelate ring are formed less and exhibit the first d-d absorption band, $^1A_{1g}\rightarrow{}^1T_{1g}$ (O_h), at lower energy than the other isomers. The results may be attributed to the steric effect; the isomers with the *N*-methyl group disposed over the tp chelate ring are more crowded and would be less stable than the isomers with the hydrogen atom in place of the methyl group. Similar relationships among the structure, isomer distribution, and d-d band energy were observed for the corresponding ox[2] and acac[15] complexes. The

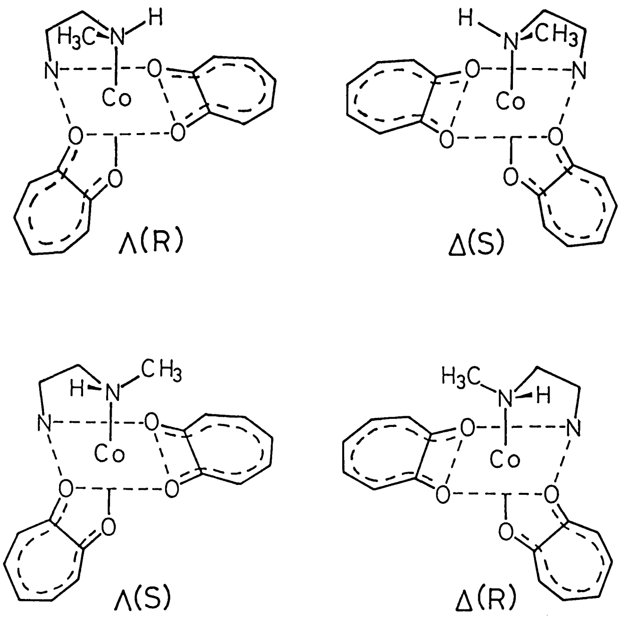

Fig. 1. The four stereoisomers of $[Co(tp)_2(Me\text{-}en)]^+$.

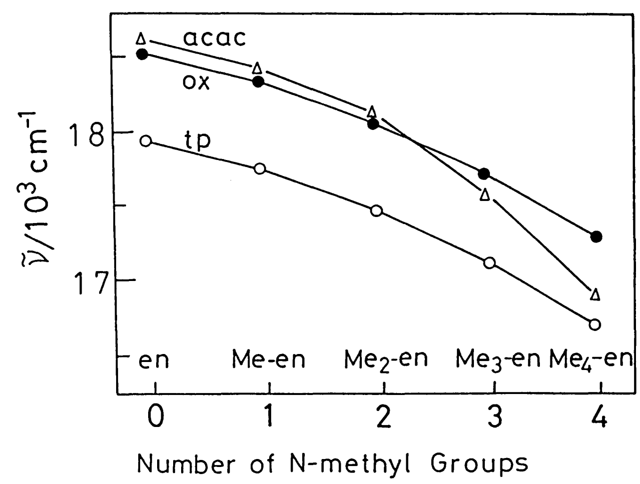

Fig. 2. Correlation between the positions of the first d-d absorption band of $[Co(tp)_2(R^1R^2NCH_2CH_2NR^3R^4)]^+$($R^1$—$R^4$=H or CH_3), $[Co(ox)_2(R^1R^2NCH_2CH_2NR^3R^4)]^-$, and $[Co(acac)_2(R^1R^2NCH_2CH_2NR^3R^4)]^+$, and the number of *N*-methyl groups of the diamine ligand.

Table 5. ^{1}H NMR and Absorption Spectral Data for $[Co(tp)_2(diamine)]^+$ and the Distributions of the Isomers at Equilibrium (34 °C)

Diamine	Assignment	^{1}H NMR (δ)		Absorption	Relative
		CH₃	N<u>H</u>(CH₃)	$\tilde{\nu}_{max}/10^3\ cm^{-1}$ ($\log\varepsilon$)	abundance/%
en				17.92(2.39) 26.88(4.13) 29.33(4.23) 41.32(4.81)$^{c)}$	
Me-en	$\Lambda(R)\Delta(S)$	2.44d	5.64$^{a)}$	17.73(2.38) 26.81(4.15) 29.33(4.24) 41.32(4.84)$^{d)}$	69
	$\Lambda(S)\Delta(R)$	1.84d	6.15$^{a)}$	17.67(2.38) 26.81(4.13) 29.33(4.24) 41.32(4.85)$^{d)}$	31
N,N'-Me₂-en	$\Lambda(RR)\Delta(SS)$	2.37d	5.75$^{a)}$	17.61(2.34) 26.74(4.13) 29.33(4.22) 41.32(4.85)$^{d)}$	58
	$\Lambda(RS)\Delta(SR)$	2.41d 1.73d	5.74 6.62$^{a)}$	17.48(2.29) 26.67(4.09) 29.33(4.18) 41.32(4.82)$^{d)}$	23
	$\Lambda(SS)\Delta(RR)$	1.73d	6.76$^{a)}$	17.42(2.33) 26.60(4.09) 29.31(4.17) 41.32(4.82)$^{d)}$	19
N,N-Me₂-en		2.64s 1.83s$^{b)}$		17.18(2.32) 26.53(4.12) 29.24(4.24) 41.15(4.81)$^{c)}$	
Me₃-en	$\Lambda(R)\Delta(S)$	2.62s 2.37d 1.82s	5.94$^{a)}$	17.06(2.31) 26.46(4.12) 29.24(4.24) 41.15(4.85)$^{d)}$	82
	$\Lambda(S)\Delta(R)$	2.64s 1.75d 1.81s	6.86$^{a)}$	17.00(2.31) 26.46(4.10) 29.24(4.19) 41.15(4.82)$^{d)}$	18
Me₄-en		2.63s 1.82s$^{b)}$		16.61(2.23) 26.32(4.02) 29.24(4.13) 40.98(4.74)$^{c)}$	

a) In CD_3OD–DCl. b) In CD_3OD. c) In H_2O. d) In 10^{-2} M HCl.

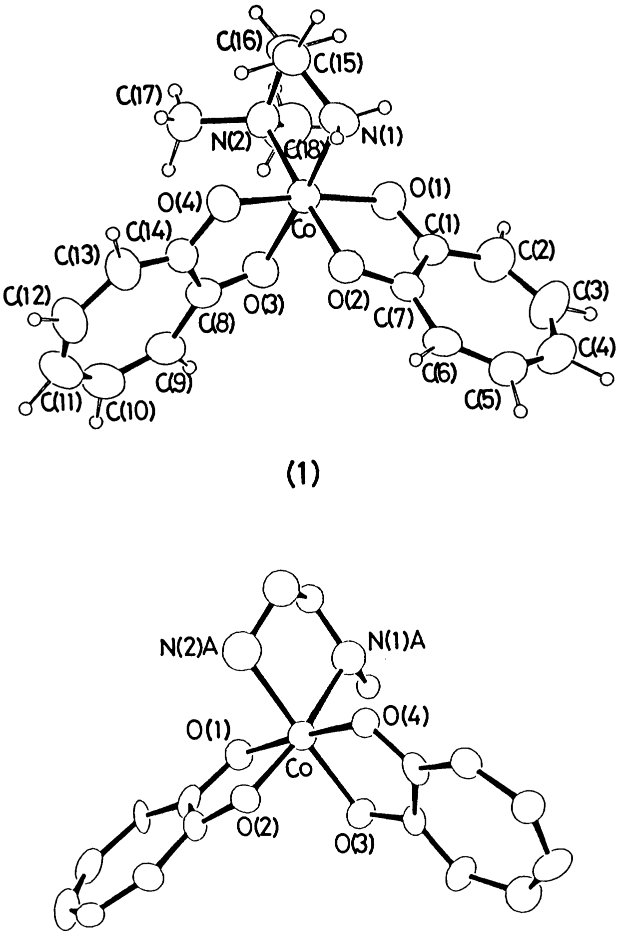

Fig. 3. Perspective views of $[Co(tp)_2(N,N\text{-}Me_2\text{-}en)]^+$ (**1**) and $\Lambda(R)\Delta(S)$-$[Co(tp)_2Me\text{-}en)]^+$ (the $\Delta(S)$ isomer is shown).

Table 6. Electrochemical Data for the Reduction of $[Co(tp)_2(diamine)]^+$ (vs. SCE) at 24 °C[a)]

Complex	$E_{1/2}/V$	$\lvert E_{3/4}-E_{1/4}\rvert/V$[b)]
$[Co(tp)_2(en)]^+$	−0.31	0.100
$\Lambda(R)\Delta(S)$-$[Co(tp)_2(Me\text{-}en)]^+$	−0.37	0.095
$\Lambda(RR)\Delta(SS)$-$[Co(tp)_2(N,N'\text{-}Me_2\text{-}en)]^+$	−0.40	0.095
$[Co(tp)_2(N,N\text{-}Me_2\text{-}en)]^+$	−0.20	0.095
$\Lambda(R)\Delta(S)$-$[Co(tp)_2(Me_3\text{-}en)]^+$	−0.24	0.095
$[Co(tp)_2(Me_4\text{-}en)]^+$	−0.09	0.095

a) By glassy carbon rotating disk experiments (in 0.1 M KCl–0.001 M $HClO_4$ with a 0.01 $V\,s^{-1}$ scan rate; 2000 rev min^{-1}). b) $E_{3/4}$ and $E_{1/4}$ are potentials at three-fourth and one-fourth of the limiting current value, respectively.

first d–d band shifts to lower energy similarly to those of the ox and acac complexes as the number of methyl substituents on the nitrogen atom increases (Fig. 2). The second d–d band, $^1A_{1g}\rightarrow{}^1T_{2g}$ (O_h), is hidden by the charge-transfer bands. Figure 2 demonstrates that the ligand field strength of the tp chelate is smaller than those of the acac and ox chelates.

Structures of $[Co(tp)_2(N,N\text{-}Me_2\text{-}en)]ClO_4$ (1) and $\Lambda(R)\Delta(S)$-$[Co(tp)_2(Me_2\text{-}en)]ClO_4$ (2). Perspective drawings of the complex cations are presented in Fig. 3. The Co–N(1) and Co–N(2) bond lengths in (**1**) are 1.930(3) and 2.022(4) Å, respectively. The longer bond distance at the tertiary amine nitrogen-atom side is attributed to the steric repulsion between the methyl groups and other ligands in the complex. The short contacts involving the methyl carbon atoms are C(17)···O(4) = 2.86(1) Å and C(18)···O(1) = 2.86(1) Å. The five-membered chelate ring of *N*, *N*-Me_2-en takes an envelope form with two N-CH_3 bond axes in intermediate directions between axial and equatorial. The geometries of the tropolonate ions agree with those reported for $[Co(tp)_3]$.[16)] In the crystals of (**2**), the complex cation takes two possible orientations, which are related by the pseudo-two-fold axis passing through the Co atom and the midpoint of the C–C bond in the Me-en chelate ring. The same type of the disorder was observed in the crystals of $[Co(en)(tn)(tmd)][Co(CN)_6]\cdot H_2O$ (tn = trimethylenediamine, tmd = tetramethylenediamine).[17)] The complex cation in (**2**) is the $\Lambda(R)\Delta(S)$ isomer. The assignment by the ^1H NMR spectra was confirmed. Unfortunately, the low accuracy of the structural data prevented the observation of the effect of the *N*-methyl group on the Co–N(secondary amine) bond distance.

Electrochemistry. Electrochemistry is very useful for evaluating electronic effects of substituents on the ligand in metal complexes. In the present complexes, electrochemistry allows us to assess the electronic contributions of the added methyl groups. Rotating glassy carbon electrode voltammograms of the tp complexes were obtained in 10^{-1} M KCl–10^{-3} M $HClO_4$ vs. a saturated calomel electrode (SCE), and the results are summarized in Table 6. The complexes show a quasi-reversible reduction wave assignable to the Co^{3+}/Co^{2+} couple. The half-wave potentials ($E_{1/2}$ values) range from −0.09 V to −0.40 V. The difference in $E_{1/2}$ between the isomers is small in each complex. The inductive action accompanying the replacement of H with CH_3 would donate more electron density on the cobalt atom. Thus, the inductive effect alone would shift the $E_{1/2}$ value systematically to more negative (more difficult to reduce) as the number of methyl groups increases. The data in Table 6, however, can not be explained by a simple inductive effect due to the added methyl groups. For example, the increase in potential of 0.11 V as one goes from $[Co(tp)_2(en)]^+$ (−0.31 V) to $[Co(tp)_2(N,N\text{-}Me_2\text{-}en)]^+$ (−0.20 V) does not agree with the expected increase in electron density on the metal upon replacing H with CH_3. The apparent discrepancy may be related to the steric effect of -$N(CH_3)_2$. As described above, the X-ray analysis of $[Co(tp)_2(N,N\text{-}Me_2\text{-}en)]^+$ shows that the Co–N(tertiary amine) bond length (2.022(4) Å) is longer than the Co–N(primary amine) one (1.930(3) Å). The longer bond length implies a weaker bond and smaller donation of electron density from N to Co. However, the $E_{1/2}$ values for the Me-en and *N,N'*-Me-en complexes suggest that the NH(CH$_3$) group is more electron-donating than the NH$_2$ group as expected from the inductive effect. The data in Table 6 show that the replacement of $-NH_2$ with $-NH(CH_3)$ shifts the reduction potential in the cathodic direction by ca. 50 mV, while that with $-N(CH_3)_2$ in the anodic direction by ca. 100 mV, and that the additivity between the two contributions holds. It is to be noted, however, that the first d–d absorption band shifts progressively to lower energy as the number of methyl substituents on the nitrogen atom increases. We have no explanation for this discrepancy at present.

Racemization of [Co(tp)$_2$(en)]$^+$. Metal chelates are classified into two categories, slow and fast in terms of their rearrangement rates.[18] Cobalt(III) chelates fall under the category of slow complexes. However, cobalt(III)-tropolonates, [Co(α-C$_3$H$_5$tp)$_3$] (α-C$_3$H$_5$tp= α-isopropenyltropolonate) and [Co(α-C$_3$H$_7$tp)$_3$] (α-C$_3$H$_7$tp=α-isopropyltropolonate) are reported to be stereochemically nonrigid.[5] For example, the inversion ($\Lambda \rightleftarrows \Delta$) rate of mer-[Co($\alpha$-C$_3H_5$tp)$_3$] at 25 °C, k=100 s^{-1}, is ca. 10^{11} times greater than that of [Co(acac)$_3$] at the same temperature and a trigonal-twist mechanism was proposed.[5] Thus it is interesting to study the racemization (inversion) rates of bis(tropolonato)cobalt(III) complexes. The rate of racemization of [Co(tp)$_2$(en)]$^+$ was measured at pH 2.8 and 7.2 (70 °C, Fig. 4). The rate was independent of pH. No detectable change in absorption spectrum was observed during the racemization. The rate constant (6.4×10^{-4} s^{-1} at 70 °C) is ca. 10^7 times smaller than that for [Co(α-C$_3$H$_7$tp)$_3$].

Deuteration and Epimerization Reactions. Kinetic studies of reversible isomerization (epimerization) between the two isomers ($\Lambda(S)\Delta(R)$ and $\Lambda(R)\Delta(S)$) of [Co(tp)$_2$(Me-en or Me$_3$-en)]$^+$ were performed in aqueous solutions at 34.0 °C by observing the change in chromatograms with reaction time. Kinetic data are

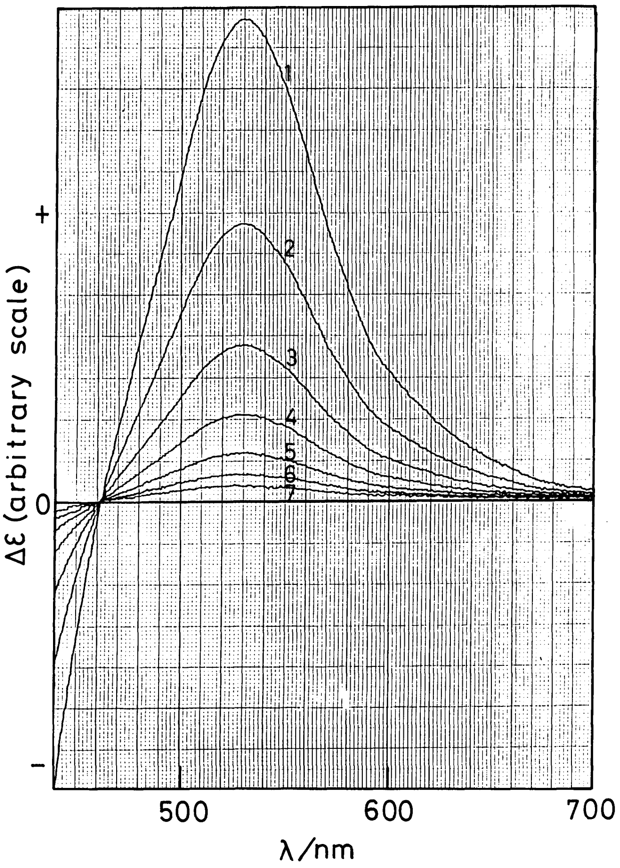

Fig. 4. Change in CD spectrum of $(+)^{CD}_{530}$-[Co(tp)$_2$(en)]$^+$ in water at pH 7.2 and 70 °C. Spectra 1—7 were measured every 15 min.

Table 7. Rate Constants for the Deuteration and Inversion at the Chiral Nitrogen Centers of [Co(tp)$_2$(Me-en or Me$_3$-en)]$^+$ at 34.0 °C

Complex	Isomer	pD	$k_{D(obsd)}$/s^{-1}	k_D/M^{-1}s^{-1}
[Co(tp)$_2$(Me-en)]$^+$	$\Lambda(R)\Delta(S)$	6.25	5.6×10^{-5}	1.2×10^4
		6.67	1.4×10^{-4}	1.1×10^4
		6.85	2.1×10^{-4}	1.1×10^4
	$\Lambda(S)\Delta(R)$	6.05	1.7×10^{-4}	5.7×10^4
		6.26	2.8×10^{-4}	5.8×10^4
		6.67	7.1×10^{-4}	5.8×10^4
[Co(tp)$_2$(Me$_3$-en)]$^+$	$\Lambda(R)\Delta(S)$	5.71	2.2×10^{-5}	1.7×10^4
		6.10	5.7×10^{-5}	1.7×10^4
		6.67	2.1×10^{-4}	1.7×10^4
	$\Lambda(S)\Delta(R)$	5.55	1.4×10^{-4}	1.5×10^5
		6.10	5.1×10^{-4}	1.5×10^5
		6.42	1.0×10^{-3}	1.4×10^5

Complex	pH	$k_{ep(obsd)}$/s^{-1}	k_{ep}/M^{-1}s^{-1}
[Co(tp)$_2$(Me-en)]$^+$	8.49	3.7×10^{-4}	6.1×10
	8.89	9.7×10^{-4}	6.4×10
	9.33	2.6×10^{-4}	6.3×10
[Co(tp)$_2$(Me$_3$-en)]$^+$	7.32	2.9×10^{-4}	7.0×10^2
	7.77	8.3×10^{-4}	7.2×10^2
	8.04	1.5×10^{-3}	6.9×10^2

summarized in Table 7. For each complex, the $k_{ep(obsd)}/[OH^-]$ ($=k_{ep}$) values are constant at 34.0 °C in the pH range measured, indicating that the reaction is first order in $[OH^-]$. Thus, the rate law was the same as that obtained previously for other amine complexes, $R=k_{ep}[\text{complex}][OH^-]$.[19] Since the rate of inversion at cobalt in $[Co(tp)_2(en)]^+$ is very slow and is independent of pH (vide supra), the Me-en and Me$_3$-en complexes are believed to epimerize by inversion at the chiral nitrogen atoms. The rates of deuteration at the chiral nitrogen centers of $[Co(tp)_2(Me\text{-}en)]^+$, and $[Co(tp)_2(Me_3\text{-}en)]^+$ were followed by monitoring signal changes in the ^{1}H NMR spectra; the N–CH$_3$ doublet signal becomes a singlet by deuteration. From the spectral changes, the pseudo first-order rate constants for deuteration, $k_{D(obsd)}$ were obtained as described previously.[9] The rate law for the deuteration reaction was the same as that obtained for other amine complexes, $R=k_D[\text{complex}]\ [OD^-]$.[19] The $k_{D(obsd)}$ and k_D values are given in Table 7. Table 8 compares the k_{ep} and k_D values for the tp complexes with those for the corresponding acac and ox complexes. We assume here that the proton-exchange (deuteration) and epimerization ($\Lambda(S)\rightleftarrows\Lambda(R)$) reactions proceed by Eqs. 1—3.

$$\Lambda(S)\text{-}[Co(tp)_2(NH(CH_3)CH_2CH_2NH_2)]^+ + OH^- \underset{k_{+H^+}}{\overset{k_{-H^+}}{\rightleftarrows}} \Lambda(S)\text{-}[Co(tp)_2(^-N(CH_3)CH_2CH_2NH_2)] + H_2O \quad (1)$$

$$\Lambda(S)\text{-}[Co(tp)_2(^-N(CH_3)CH_2CH_2NH_2)] \underset{k'_i}{\overset{k_i}{\rightleftarrows}} \Lambda(R)\text{-}[Co(tp)_2(^-N(CH_3)CH_2CH_2NH_2)] \quad (2)$$

$$\Lambda(R)\text{-}[Co(tp)_2(^-N(CH_3)CH_2CH_2NH_2)] + H_2O \underset{k'_{-H^+}}{\overset{k'_{+H^+}}{\rightleftarrows}} \Lambda(R)\text{-}[Co(tp)_2(NH(CH_3)CH_2CH_2NH_2)]^+ + OH^- \quad (3)$$

The actual rate of inversion of the amido complex is k_i (k'_i) and is pH independent.[20] The measured rate constant for epimerization (k_{ep}) is pH dependent since the rate depends on the amount of amido complex present. If the reprotonation rate is constant (diffusion controlled) as has been estimated for other cobalt(III)–amine complexes, differences in observed proton-exchange rates (k_D) result strictly from a difference in proton dissociation constants (K_a) of the complexes.[19]

It is known that deuteration rates increase with an increasing positive charge on the complex as expected on the basis of electrostatic consideration.[1] Thus the unipositive tp and acac complexes are expected to give larger k_D values than the uninegative ox complexes. However, the inverse has been found. The results suggest that the reactivity of coordinated secondary amine nitrogen center is affected more by the kind of coexisting ligands than the overall charge on the complex. As we suggested previously,[2] the small rates of the tp and acac complexes may be related to delocalized π-electrons in the chelate rings.

For the tp, ox, and acac complexes, the complexes with Me$_3$-en have larger k_D values than those with Me-en. The result seems to be related to a difference in electron density on the secondary amine hydrogen atoms as suggested in the ^{1}H NMR spectra. For example, as one goes from $\Lambda(S)\Delta(R)$-$[Co(tp)_2(Me\text{-}en)]^+$ to $\Lambda(S)\Delta(R)$-$[Co(tp)_2(Me_3\text{-}en)]^+$, the amine proton signal (N$\underline{H}$(CH$_3$)) is shifted from 6.15 to 6.86 ppm, suggesting a decrease in electron density on the hydrogen atom in line with the increase in k_D value.

The k_D values for the $\Lambda(S)\Delta(R)$ isomers of the tp complexes are larger than those for the $\Lambda(R)\Delta(S)$ isomers. The rate difference can be attributed to a difference in steric effect between the isomers. As is seen in Fig. 1 the secondary amine hydrogen in the $\Lambda(R)\Delta(S)$ isomer, which is situated over one of the tp ligands, will be more effectively hindered by the tp ring from attacking of OH$^-$ than the hydrogen in the $\Lambda(S)\Delta(R)$ isomer. The same interpretation is given for the rate differences between the isomers of the acac and ox complexes.

The $k_D/(k_1$ or $k_{-1})$ ratios (retention ratios) for $[Co(acac)_2(Me\text{-}en$ or $Me_3\text{-}en)]^+$ (ca. 10^4—10^5) are larger than those for $[Co(tp)_2(Me\text{-}en$ or $Me_3\text{-}en)]^+$ (ca. 10^2—10^3) and $[Co(ox)_2(Me\text{-}en$ or $Me_3\text{-}en)]^-$ (ca. 10^2), and the large

Table 8. A Comparison of Data for the Deuteration and Inversion at the Chiral Nitrogen Centers of $[Co(tp)_2L]^+$ (L=Me-en, Me$_3$en), $[Co(acac)_2L]^+$, and $[Co(ox)_2L]^-$ at 34.0 °C

Complex	Isomer	$k_D/M^{-1}s^{-1}$	$k_{ep}/M^{-1}s^{-1}$	$(k_1$ or $k_{-1})/M^{-1}s^{-1}$	$k_D/(k_1$ or $k_{-1})$
$[Co(tp)_2(Me\text{-}en)]^+$	$\Lambda(R)\Delta(S)$	1.1×10^4	6.3×10	k_{-1}: 2.0×10	5.5×10^2
	$\Lambda(S)\Delta(R)$	5.8×10^4		k_1: 4.3×10	1.3×10^3
$[Co(tp)_2(Me_3\text{-}en)]^+$	$\Lambda(R)\Delta(S)$	1.7×10^4	7.0×10^2	k_{-1}: 1.3×10^2	1.3×10^2
	$\Lambda(S)\Delta(R)$	1.5×10^5		k_1: 5.7×10^2	2.6×10^2
$[Co(acac)_2(Me\text{-}en)]^+$ a)	$\Lambda(R)\Delta(S)$	c)	1.3×10^{-1}	k_{-1}: 5.9×10^{-2}	
	$\Lambda(S)\Delta(R)$	8.9×10^3		k_1: 7.1×10^{-2}	1.3×10^5
$[Co(acac)_2(Me_3\text{-}en)]^+$ b)	$\Lambda(R)\Delta(S)$	2.4×10^3	1.0	k_{-1}: 3.4×10^{-1}	7.1×10^3
	$\Lambda(S)\Delta(R)$	1.1×10^4		k_1: 6.6×10^{-1}	1.7×10^4
$[Co(ox)_2(Me\text{-}en)]^-$ b)	$\Lambda(R)\Delta(S)$	2.2×10^4	8.4×10^2	k_{-1}: 2.7×10^2	8.1×10
	$\Lambda(S)\Delta(R)$	1.8×10^5		k_1: 5.7×10^2	3.2×10^2
$[Co(ox)_2(Me_3\text{-}en)]^-$ b)	$\Lambda(R)\Delta(S)$	1.2×10^5	1.2×10^4	k_{-1}: 2.1×10^3	5.7×10
	$\Lambda(S)\Delta(R)$	8.1×10^5		k_1: 9.9×10^3	8.2×10

a) From Ref. 8. b) From Ref. 2. c) The data could not be obtained because of the overlapping of the N–CH$_3$ and C–CH$_3$ signals.

values imply that the configuration about the chiral nitrogen atom (pyramidal configuration) is retained most of the time when the proton is off the quarternary N site. However, the factors controlling the retention ratios for the above complexes are not clear at the moment.

The present work was partially supported by a Grant-in-Aid for Scientific Research No. 03453051 from the Ministry of Education, Science and Culture.

References

1) J. W. Palmer and F. Basolo, *J. Phys. Chem.*, **64**, 778 (1960).

2) G. Ma, T. Hibino, M. Kojima, and J. Fujita, *Bull. Chem. Soc. Jpn.*, **62**, 1053 (1989).

3) H. Kawaguchi, M. Matsuki, T. Ama, and T. Yasui, *Bull. Chem. Soc. Jpn.*, **59**, 31 (1986).

4) B. Halpern, A. M. Sargeson, and K. R. Turnbull, *J. Am. Chem. Soc.*, **88**, 4630 (1966).

5) S. S. Eaton, J. R. Hutchison, R. H. Holm, and E. L. Muetterties, *J. Am. Chem. Soc.*, **94**, 6411 (1972).

6) M. Shibata, *Nippon Kagaku Zasshi*, **87**, 771 (1966).

7) M. Fujita, Y. Yoshikawa, and H. Yamatera, *Chem. Lett.*, **1982**, 437.

8) P. K. Glasoe and F. A. Long, *J. Phys. Chem.*, **64**, 188 (1960).

9) M. Kojima, T. Hibino, Y. Ouyang, and J. Fujita, *Inorg. Chim. Acta*, **117**, 1 (1986).

10) W. R. Busing and H. A. Levy, *Acta Crystallogr.*, **10**, 180 (1957).

11) P. Main, S. E. Hull, L. Lessinger, G. Germain, J. -P. Declercq, and M. M. Woolfson, MULTAN 78. A system of Computer Programs for the Automatic Solution of Crystal Structures from X-ray Diffraction Data. Univs. of York, England, and Louvain, Belgium (1978).

12) "International Tables for X-Ray Crystallography," Birmingham, Kynoch Press (1974), Vol. IV. (Present distributor D. Reidel, Dordrecht.)

13) T. Sakurai and K. Kobayashi, *Rikagaku Kenkyusho Hokoku*, **55**, 69 (1979).

14) Tables of the coordinates of hydrogen atoms of (**1**), the bond lengths and bond angles of (**2**), the anisotropic thermal parameters of the non-hydrogen atoms, and the observed and calculated structure factors are deposited as Document No. 9001 at the Office of the Editor of Bull. Chem. Soc. Jpn.

15) Y. Ouyang, M. Kojima, and J. Fujita, *Bull. Chem. Soc. Jpn.*, **57**, 3574 (1984).

16) D. M. Doddrell, M. R. Bendall, P. C. Healy, G. Smith, C. H. L. Kennard, C. L. Raston, and A. H. White, *Aust. J. Chem.*, **32**, 1219 (1979).

17) H. Takazawa, S. Ohba, Y. Saito, H. Ichida, and K. Rasmussen, *Acta Crystallogr., Sect. C*, **46**, 2354 (1990).

18) J. G. Gordon, II and R. H. Holm, *J. Am. Chem. Soc.*, **92**, 5319 (1970); J. R. Hutchison, J. G. Gordon, II, and R. H. Holm, *Inorg. Chem.*, **10**, 1004 (1971).

19) W. G. Jackson and A. M. Sargeson, "Rearrangement in Coordination Complexes," in "Rearrangements in Ground and Excited States," ed by P. de Mayo, Academic Press, New York (1980), Vol. 2, p. 273, and references therein.

20) T. P. Pitner and R. B. Martin, *J. Am. Chem. Soc.*, **93**, 4400 (1971).

21) J. W. Palmer and F. Basolo, *J. Inorg. Nucl. Chem.*, **15**, 279 (1960).